Optimal detuning in optically pumped 10<bold>λ</bold> ultraviolet vertical-cavity surface-emitting lasers for temperature stability and low

Applied Physics Letters

RESEARCH ARTICLE | DECEMBER 18 2025

Optimal detuning in optically pumped 10λ ultraviolet vertical-cavity surface-emitting lasers for temperature stability and low threshold

E. Torres ; J. Ciers ; S. Graupeter ; T. Wernicke ; M. Kneissl ; Å. Haglund

Appl. Phys. Lett. 127, 241104 (2025)
https://doi.org/10.1063/5.0283588

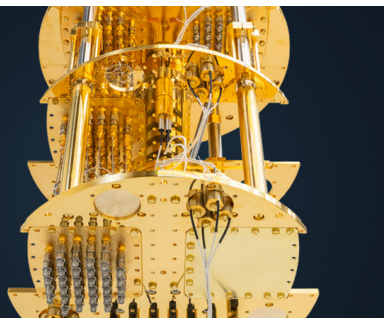

AIP Publishing

Applied Physics Letters ARTICLE pubs.aip.org/aip/apl

Optimal detuning in optically pumped 10λ ultraviolet vertical-cavity surface-emitting lasers for temperature stability and low threshold

Cite as: Appl. Phys. Lett. **127**, 241104 (2025); doi: 10.1063/5.0283588
Submitted: 2 June 2025 · Accepted: 28 November 2025 ·
Published Online: 18 December 2025

E. Torres,[1,a)] J. Ciers,[1] S. Graupeter,[2] T. Wernicke,[2] M. Kneissl,[2,3] and Å. Haglund[1]

AFFILIATIONS

[1]Department of Microtechnology and Nanoscience, Chalmers University of Technology, 41296 Gothenburg, Sweden
[2]Institute of Solid State Physics, Technische Universität Berlin, 10623 Berlin, Germany
[3]Ferdinand-Braun-Institut (FBH), 12489 Berlin, Germany

[a)]Author to whom correspondence should be addressed: estrella@chalmers.se

ABSTRACT

In vertical-cavity surface-emitting lasers (VCSELs), the lasing wavelength is defined by the longitudinal cavity mode. The spectral misalignment between the resonance wavelength and the gain peak, known as detuning, is crucial for the device performance. Temperature also influences detuning since the gain peak red shifts faster than the resonance wavelength when the temperature increases. These important effects have not been explored in detail for ultraviolet (UV) VCSELs despite the significant heating that is expected due to high electrical resistance and high thermal impedance. Here, we studied the threshold and detuning dependence in optically pumped AlGaN-based UVB and UVC VCSELs with different cavity lengths operated at different temperatures. The cavity lengths of the VCSELs, fabricated from the same epitaxial material, are varied by post-growth deposition of HfO_2 spacer layers with different thicknesses. The results show a strong relation between the threshold and the detuning, where VCSELs have thresholds around 5 MW/cm^2 for a nominal (operational) detuning of −2.5 nm (∼−1 nm), and below 1 MW/cm^2 when the nominal (operational) detuning is set between 2 and 3 nm (1–3 nm) with a minimum threshold of 0.23 MW/cm^2. Additionally, the temperature dependence of the VCSELs' thresholds is investigated and compared by temperature-dependent photoluminescence and an empirical relation. The VCSELs with lower thresholds at room temperature are, on average, 20 times less sensitive to temperature than those with higher thresholds at room temperature, suggesting that VCSELs with a nominal detuning of 2–3 nm are the optimum design choice.

There is growing interest in replacing conventional but toxic medium- and low-pressure ultraviolet (UV) Hg lamps as well as bulky and low-efficient UVC excimer and solid-state lasers. AlGaN-based emitters, such as UV light-emitting-diodes (LEDs) as well as edge-emitting lasers (EELs) where both UVB[1] and UVC[2] EELs have been achieved, provide alternative UV-light sources.[3] UV vertical-cavity surface-emitting lasers (VCSELs) offer the advantages of circular-symmetric low-divergent output beams, low threshold currents, high modulation frequencies at low currents, and 2D integration capability.[4] This could be useful for solar-blind communication systems where the low divergent output beam and modulation speed of VCSELs could be an interesting alternative to the actual UV LED panels employed.[5] Furthermore, VCSELs' far fields result in low coupling losses and are suitable for gas sensors that require optical fibers or charge management systems.[6] Nevertheless, the fabrication of a VCSEL in the UV is not straightforward, and no electrically injected UV VCSEL has yet been demonstrated.

Hurdles in VCSEL fabrication include, for instance, the achievement of highly reflective distributed Bragg reflectors (DBRs). Mainly, dielectric SiO_2/HfO_2 DBRs have shown reflectivity above 99 % even at wavelengths below 250 nm[7] and have been successfully used to demonstrate all optically pumped UVB[8,9] and UVC[10–12] VCSELs. However, VCSELs with all-dielectric DBRs require substrate removal to access both cavity surfaces. This is a critical step that should ideally provide cavity length control and smooth exposed surfaces, which has been shown by both electrochemical etching[9,13] and photo-assisted electrochemical etching.[12]

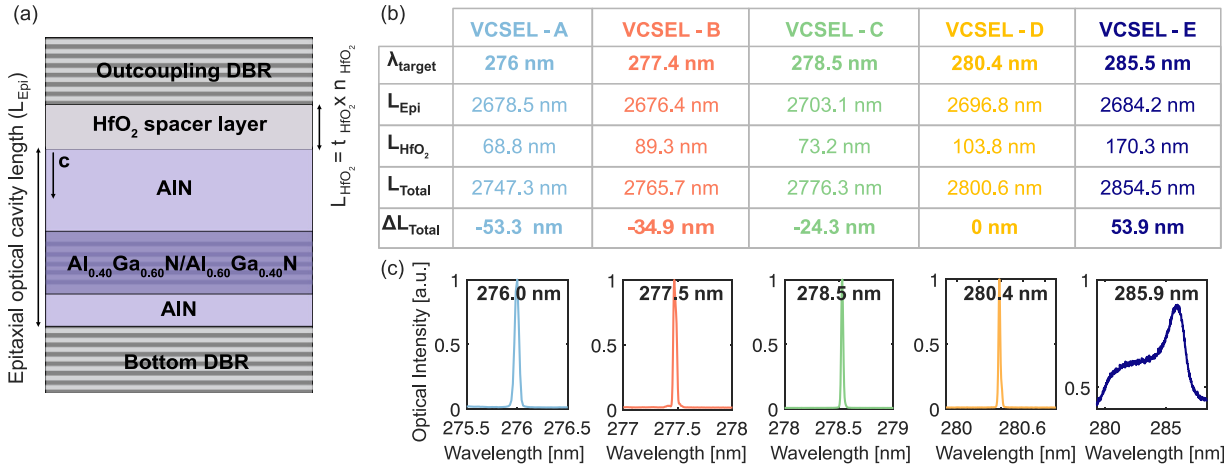

	VCSEL - A	VCSEL - B	VCSEL - C	VCSEL - D	VCSEL - E
λ_{target}	276 nm	277.4 nm	278.5 nm	280.4 nm	285.5 nm
L_{Epi}	2678.5 nm	2676.4 nm	2703.1 nm	2696.8 nm	2684.2 nm
L_{HfO_2}	68.8 nm	89.3 nm	73.2 nm	103.8 nm	170.3 nm
L_{Total}	2747.3 nm	2765.7 nm	2776.3 nm	2800.6 nm	2854.5 nm
ΔL_{Total}	-53.3 nm	-34.9 nm	-24.3 nm	0 nm	53.9 nm

FIG. 1. (a) Side-view representation of a UVC VCSEL where the epitaxial optical cavity length (L_{Epi}) and optical HfO_2 spacer length (L_{HfO_2}) are indicated by the black arrows. The physical thickness of HfO_2 is denoted by (t_{HfO_2}) and the refractive index by (n_{HfO_2}). (b) Table describing the targeted lasing wavelength (λ_{target}) and optical cavity lengths of VCSELs-A, VCSELs-B, VCSELs-C, VCSELs-D, and VCSELs-E. The total optical cavity length (L_{Total}) is the sum of L_{growth} and L_{HfO_2}. ΔL_{Total} refers to the difference between L_{Total} of VCSEL-D and L_{Total} of the other VCSELs. (c) From left to right, photoluminescence spectra of VCSEL-A, VCSEL-B, VCSEL-C, VCSEL-D, and VCSEL-E, where all devices are pumped at $1.5 \times P_{th}$, except for VCSEL-E, which is pumped at 30 MW/cm^2.

The importance of cavity length control is related to the short cavity of VCSELs, which usually is on the order of a few wavelengths (λ) and consequently presents a large mode spacing, allowing only a few resonances to overlap with the gain medium. Hence, the lasing emission is set by the resonance that experiences the highest net gain. The quantification of the spectral misalignment of the cavity resonance and gain peak is called detuning and strongly influences the device threshold. For instance, Cardinali *et al.*[9] showed that a physical cavity length variation of $\sim$10 nm in 2.5 λ-cavity UVB VCSELs led to an increase in threshold pump power density of a factor of 10, and Watanabe *et al.* achieved blue GaN-based VCSELs with wall plug efficiencies over 20 % by controlling the cavity length using *in situ* reflectivity spectra measurements during the growth.[14] However, contrary to an EEL, the gain spectrum is difficult to measure in VCSELs, and there have been only very few attempts using the Hakki–Paoli method for long-cavity GaN-based VCSELs.[15] Therefore, the spontaneous emission peak of the quantum wells (QWs) is commonly used, instead of the spectral position of the gain peak, to define the detuning between the resonance wavelength and the gain peak.

However, III-nitride QWs typically have a very strong blue shift of the photoluminescence (PL) peak with increasing pump power density due to screening of the quantum confined Stark effect and band filling, and the detuning therefore varies with pump power density. We will here define two different detuning values: operational detuning, which is the difference between the lasing wavelength (λ_{lasing}) and the QWs peak emission (λ_{QWs}) at the threshold pump power density (P_{th}), see Eq. (1), and nominal detuning at room temperature, which uses λ_{QWs} at 1 MW/cm^2, see Eq. (2),

$$\text{Operational detuning} = \lambda_{lasing}(T) - \lambda_{QWs}(P_{th}, T), \quad (1)$$

$$\text{Nominal detuning} = \lambda_{lasing} - \lambda_{QWs}(1\,\text{MW/cm}^2). \quad (2)$$

The former is useful for understanding the physics of the devices, but the latter is useful from a design point of view when the threshold of your laser is unknown. Note that when the threshold is reached, the carrier concentration is clamped and the PL should not shift significantly due to carrier-induced effects. Moreover, both the lasing wavelength and PL peak are also dependent upon temperature (T), thus, temperature-induced detuning has also been included in the operational detuning calculations. In general, the cavity resonance red shifts with temperature due to the positive thermo-optic coefficient changes in the cavity. Values between 12 and 18.5 pm/K[16] have been found for GaN-based VCSELs while for UV VCSELs the available data is limited. One report on a 2.5 λ-cavity UVB VCSEL showed a wavelength shift of less than 0.1 nm over an 80 K range by employing HfO_2 with a negative thermo-optic coefficient in the DBRs.[17] However, longer cavities will be needed for electrically driven UV VCSELs to improve current spreading and thermal management, which may result in a larger wavelength shift.

The gain peak red shifts faster than the resonance wavelength and also drops in magnitude with temperature due to the reduction of the internal quantum efficiency and bandgap. Electroluminescence measurements of GaN-based VCSELs and UVB LEDs have shown red-shift rates of 30–34 pm/K.[18,19] These factors lead to temperature-induced detuning, which causes the threshold to increase.[20] The threshold can be locally approximated by a second-order polynomial function,[20]

$$P_{th}(T) = P_{\min} + \beta(T - T_{\min})^2, \quad (3)$$

where P_{min} is the minimum P_{th}, β is the temperature sensitivity factor, and T_{min} is the temperature at the minimum P_{th}. The coefficient β is related to the change in threshold with temperature, and serves as a benchmark coefficient to compare the temperature stability of different VCSELs, analogous to the characteristic temperature used in EELs. In this work, a series of UVB and UVC VCSELs with different cavity lengths is fabricated from the same epitaxial material by employing a HfO_2 spacer layer, to study the influence of temperature-dependent detuning on P_{th}.

The VCSELs consist of an AlN cavity with $5 \times Al_{0.40}Ga_{0.60}N/Al_{0.60}Ga_{0.40}N$ QWs surrounded by 40 nm $Al_{0.70}Ga_{0.30}N$ layers. The mirrors are defined by an 11-pair SiO_2/HfO_2 outcoupling DBR and a 12-pair SiO_2/HfO_2 bottom DBR. The VCSEL design and the DBR reflectance spectra are presented in Secs. 1 and 2 of the supplementary material, respectively. Further details of the fabrication can be found elsewhere.[12] To fabricate VCSELs with different detunings, the cavity length is extended in different VCSELs by sputtering a HfO_2 spacer layer of different thicknesses before depositing the outcoupling DBR, see the sketch in Fig. 1(a). HfO_2 is a suitable material to extend the cavity since HfO_2 and AlN have similar refractive indexes (2.28 for HfO_2 and 2.27 for AlN at 278.5 nm). A series of VCSELs with five different cavity lengths emitting from 276 to 286 nm have been fabricated, as described in Fig. 1(b). Despite the different optical cavity thicknesses, we estimated the VCSELs to have similar confinement factors (around 1 % for VCSELs-A to VCSELs-D and 0.9 % for VCSELs-E) due to the asymmetric placement of the QWs and extension of the cavity by the HfO_2 spacer on the thick AlN cavity side [see in Fig. 1(a)]. PL characterization was performed with a 236.5 nm diode-pumped solid-state laser with a repetition rate of 500 Hz, and a pulse duration of 925 ps. The estimated diameter (excitation spot full width at half maximum) was $\sim 10\,\mu$m when characterizing the VCSELs and $\sim 40\,\mu$m for the bare epitaxial material. The emission peak of the QWs is 278 ± 0.2 nm at 1 MW/cm^2. A detailed description of the calculation of the pump power densities, which considers the HfO_2 spacer and the outcoupling DBR transmission at the pump wavelength, can be found in Sec. 3 of the supplementary material.

The VCSELs labeled VCSEL-A, VCSEL-B, VCSEL-C, VCSEL-D, and VCSEL-E have design wavelengths of 276, 277.4, 278.5, 280.7, and 285.5 nm, respectively. Lasing was proven by measuring the change from dispersive to non-dispersive emission at the threshold in the spectrally resolved far-field emission pattern, and the narrow spectral linewidth when the devices are pumped above threshold.[12] Figure 1(c) shows the PL spectra of the devices where VCSELs-A to VCSELs-D lase with linewidths of ~50 pm for VCSEL-A and ~20 pm for the rest of the devices when pumping at $1.5 \times P_{th}$. In contrast, VCSEL-E shows no signs of lasing even when pumping as high as 30 MW/cm^2. It is worth noting that the lasing emission of all devices is very close to the targeted wavelength, showing optical cavity length deviations below 1 %, and highlighting the excellent control of our process.

Commonly, the threshold in VCSELs is determined by the kink in the non-linear optical power vs pump power characteristic. However, the kink is not always well defined, and using this method alone can mislead one to confuse lasing with, for instance, amplified spontaneous emission. Here, the threshold was estimated by the change from dispersive to non-dispersive in the spectrally resolved far-field emission pattern, as explained in Sec. 4 of the supplementary material. The estimated threshold from this method agreed well with the values obtained in the kink of the optical power pump power characteristics.

Figure 2 shows P_{th} at room temperature of all VCSELs as a function of wavelength. VCSELs-A have the highest thresholds (3.0–6.5 MW/cm^2). This can be explained by the blue shift of the PL and gain peak as a function of the pump power density (see spectra in Sec. 5 of the supplementary material) due to the band filling and screening of the quantum confined Stark effect,[21] see the solid red line in Fig. 2(a). When the active region is pumped above 3 MW/cm^2, the PL

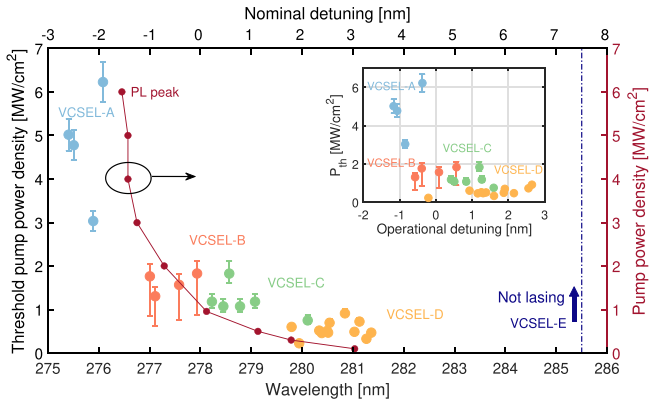

FIG. 2. Room temperature threshold pump power density for VCSELs-A, VCSELs-B, VCSELs-C, VCSELs-D, and VCSELs-E as a function of the wavelength and nominal detuning. The red solid line indicates the typical PL peak for the QWs as a function of pump power density. Inset: threshold pump power density of the VCSELs as a function of the operational detuning.

peak approaches ~276.5 nm and the calculated operational detuning at the pump power density, using Eq. (1), is reduced to values between −1.2 and −0.3 nm, as seen in the inset of Fig. 2. Following the same reasoning, VCSELs-B show operational detuning values between −1 and 1 nm and thresholds below ~2 MW/cm^2, while VCSELs-C have operational detuning values from 0 to 2 nm and thresholds around ~1.1 MW/cm^2. VCSELs-D have the lowest thresholds (below ~1 MW/cm^2) with operational detuning values between 1 and 3 nm. The minimum threshold of 0.23 MW/cm^2 is found at −0.2 nm of operational detuning. In terms of design, positive nominal detunings of 2–3 nm seem to be the most favorable to achieve VCSELs with low thresholds (VCSELs-D). To explore even larger positive detunings, VCSELs-E with thicker HfO_2 spacer layers with a nominal detuning of 7 nm were fabricated. However, these devices did not lase even at 30 MW/cm^2, probably due to extremely large detuning that prevents the lasers from obtaining enough modal gain on the long-wavelength side of the gain peak.[21] This is because the gain peak blue shifts away from the cavity resonance with increasing pump power density. These results show that the device threshold strongly depends on the operational and nominal detuning. While the lowest thresholds are achieved at positive nominal detunings (2–3 nm) as VCSELs-D show, the highest measured thresholds occur at nominal detunings of −3 to −2 nm. Note that a VCSEL with a resonance wavelength between VCSEL-D and VCSEL-E could have shown even lower thresholds. However, the fabrication of such devices was unsuccessful.

Previous detuning studies in UVB[9] showed working VCSELs with nominal detunings from −13 to 0 nm, with the lowest thresholds at a nominal detuning of around 0 to −3 nm. Even though the lowest reported thresholds are similar, with thresholds below 0.75 MW/cm^2 for VCSELs-D and 0.4 MW/cm^2 for the UVB VCSELs, the results reported here suggest a stronger impact of negative nominal detuning, as the threshold of VCSELs-A increases to ~5 MW/cm^2 for a detuning between −3 to −2 nm, whereas UVB VCSELs exhibit a similar threshold at a larger detuning of −10 nm. A possible explanation could be a larger shift of the gain peak due to the different design of the QWs allowing lasing even at a higher negative detuning. However, evidence

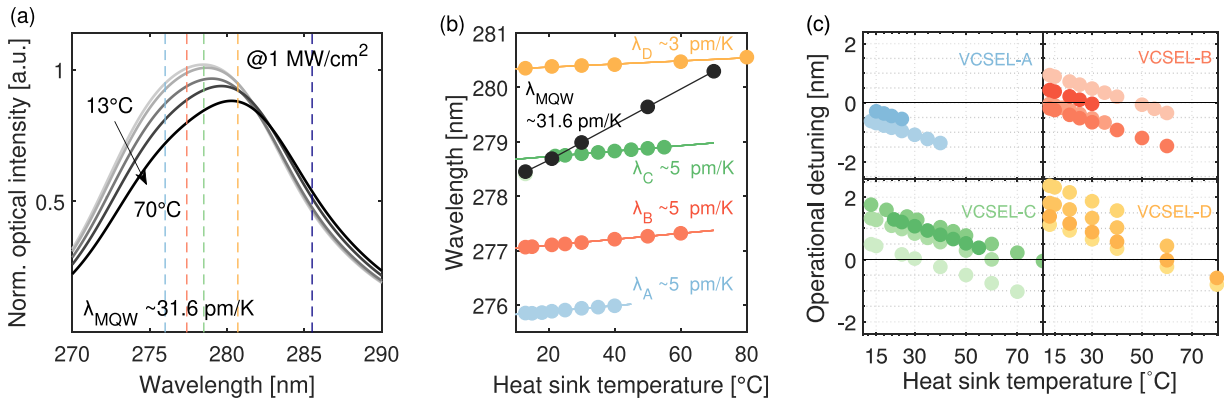

FIG. 3. (a) Temperature-dependent spontaneous emission of the QWs at 1 MW/cm^2. The dashed lines indicate the targeted wavelength of the different VCSELs at room temperature. (b) PL peak and lasing wavelength shift of one VCSEL of each kind as a function of temperature. (c) Operational temperature-induced detuning of VCSELs-A, VCSELs-B, VCSELs-C, and VCSELs-D.

for a final verdict is missing, as positive detunings were not investigated for the UVB VCSELs and gain spectra were not measured for either VCSEL structure due to the difficulty in measuring gain spectra in VCSELs.

Looking at the optical cavity length (L_{Total}) and taking VCSELs-D as a reference and optimum design, VCSELs-A with a ΔL_{Total} of −53.3 nm show, on average, thresholds 9.5 times higher. Also, P_{th} increases faster at these wavelengths because of the slower PL peak blue shift with pump power density, as shown in Fig. 2. In the other extreme, VCSELs-E with a positive ΔL_{Total} of 53.9 nm did not lase. This shows that a shorter-than-optimal cavity length, as in VCSEL-A, is less consequential, because the gain peak shifts toward the cavity wavelength at higher pump powers, allowing VCSELs-A to lase with higher thresholds. For devices with L_{Total} close to the optimum, such as VCSELs-C with a ΔL_{Total} of −24.3 nm, the threshold quickly increases by a factor of 2.2, and for VCSELs-B with a ΔL_{Total} of −34.9 nm by a factor of 3.2. Note that the reported ΔL_{Total} are optical lengths, which are roughly 2.2 times longer than the physical lengths. Thus, these findings demonstrate the sensitivity of VCSELs to cavity length variations and the need for precise control over cavity length during growth and fabrication. It should be noted that there is residual optical absorption in the HfO_2 spacer layer at the lasing wavelength, which could be a contributing factor to VCSELs-E not lasing. These have the thickest HfO_2 spacer layer of 75 nm. However, among VCSELs-A to VCSELs-D, VCSELs-D have the lowest threshold despite having the thickest HfO_2 layer of 44.5 nm among those devices, see Sec. 1 of the supplementary material. Therefore, we conclude that detuning must be the dominant factor influencing the thresholds in these 10λ cavity devices.

Temperature also impacts detuning and therefore the lasing threshold.[4] The influence of temperature can be expected to be significant in future electrically driven UV VCSELs due to the high electrical resistance and the low thermal conductivity of AlGaN and the DBRs. Thereby, we study here operational temperature-induced detuning between 13 and 80 °C by employing a Peltier element. The Joule heating during the operation of the VCSELs is negligible as a pulsed pump laser with a duty cycle of 4.6×10^{-7} (repetition rate of 500 Hz and pulse duration of 925 ps) is used. When the temperature increases, the spontaneous emission of the QWs red shifts ∼31.6 pm/K, independently of the pump power density, and drops in intensity, as shown in Fig. 3(a) at 1 MW/cm^2. Figure 3(b) shows that the lasing emission also red shifts but with a slower rate (∼5 pm/K). This red shift is associated with an increase in the refractive index due to a positive thermo-optic coefficient of the AlN cavity, which is partially compensated by the negative thermo-optic coefficient of the HfO_2 layers in the DBR and spacer layer.[17] This difference in red-shift rates between the lasing wavelength and the spontaneous emission leads to an operational temperature-dependent detuning with a negative slope, see Fig. 3(c), where the temperature further increases the operational detuning of VCSELs-A and VCSELs-B, while it decreases the absolute value of the operational detuning of some VCSELs-C and VCSELs-D as they exhibit a positive operational detuning at room temperature.

Figure 4(a) shows the temperature-dependent threshold of the different VCSELs. A clear relation is seen between the temperature-dependent P_{th} and the operational detuning at room temperature. The experimental data are fitted using Eq. (3) to compare the temperature dependencies of the devices. The fits show similar T_{min} in the range of 15–20 °C, whereas β increases strongly from VCSEL-D to VCSEL-A. The VCSEL-A type is measured over a smaller temperature range since the devices did not lase at higher temperatures, likely due to the already high P_{th} at room temperature. With an even larger operational detuning at higher temperatures, see Fig. 3(c), the modal gain is simply not sufficient to obtain lasing even when pumping at 30 MW/cm^2.

The extracted β values from the fitting are shown in Fig. 4(b). The β parameters are plotted against the nominal detuning at room temperature. This is useful to relate the impact of temperature on the VCSEL design at room temperature. A higher β indicates a faster increase in P_{th} with temperature. VCSELs-A have the highest β parameters with a maximum of 17 500 W/cm^2/°C^2, while VCSELs-D have the smallest values with a minimum of 51 W/cm^2/°C^2. Since VCSELs-D (VCSELs-A) also have the smallest (largest) P_{th} at room temperature, a direct relationship between β and P_{th} at room temperature is observed, suggesting that the design at room temperature plays an important role in determining the temperature stability. Hence, VCSELs-D with a nominal detuning of 2–3 nm show the highest temperature stability.

In summary, we have fabricated UVB and UVC VCSELs with different cavity lengths from the same epitaxial material by employing a

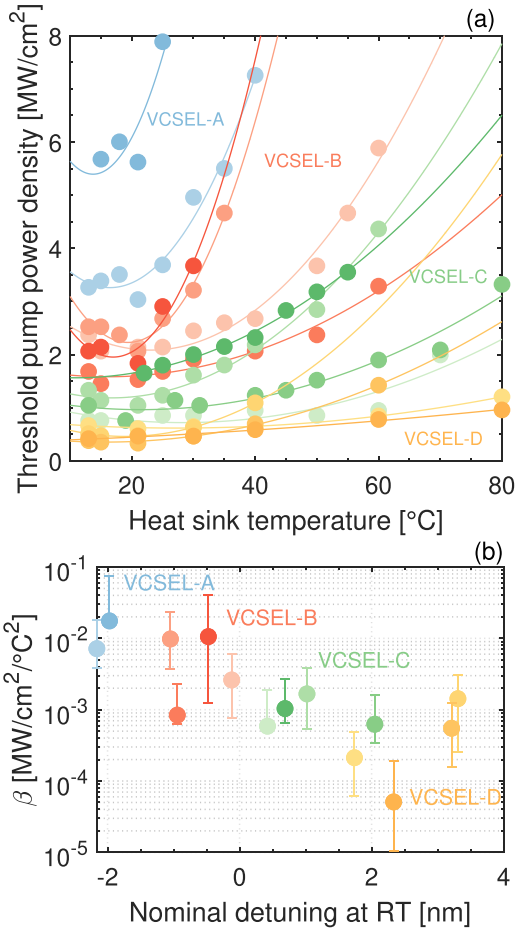

FIG. 4. (a) Threshold pump power density as a function of the temperature for VCSELs-A, VCSELs-B, VCSELs-C, and VCSELs-D. The solid lines indicate the fitting done using Eq. (1). (b) The extracted β from the fitting in (a) as a function of the nominal detuning at room temperature. The error bars represent the 95 % confidence interval.

HfO_2 spacer layer. The VCSEL-D with a target emission wavelength of 280.5 nm and a nominal (operational) detuning window of 2–3 nm (1–3 nm) shows thresholds below 0.75 MW/cm^2 with the lowest being 0.23 MW/cm^2 at room temperature. The temperature-dependent measurements show a lasing wavelength red shift of $\sim$ 5 pm/K for all VCSELs and a PL peak red shift of the QWs of $\sim$ 31.6 pm/K, inducing detuning and affecting the device threshold. VCSELs-D show the lowest β values, i.e., higher temperature stability, while VCSELs-A show the highest β, indicating that a slightly positive nominal detuning and smaller P_{th} at room temperature are more favorable for a more temperature-stable performance. Understanding the influence of detuning on threshold is helpful in the design of electrically injected UV VCSELs as excessive heating is expected due to high electrical resistance and low thermal conductivity. However, the optimum detuning is dependent on the carrier and temperature-induced gain peak shift, and thus on the active region design and operating conditions (pulsed or continuous). Therefore, a different optimum detuning can be expected in an electrically injected device.

See the supplementary material for more details on the VCSEL design, distributed Bragg reflectors, pump power density, threshold pump power density, and spontaneous emission of the quantum wells.

This work was performed in part at Myfab Chalmers University of Technology, and the project was financially supported by the European Research Council (ERC) under the European Union's Horizon 2020 research and innovation program (Grant Agreement No. 865622), the Swedish Research Council (2018-00295), and the German Federal Ministry of Education and Research (BMBF) with the "Advanced UV for life" project. The authors thank Sylvia Hagedorn from Ferdinand-Braun-Institute for providing the AlN/sapphire templates.

AUTHOR DECLARATIONS

Conflict of Interest

The authors have no conflicts to disclose.

Author Contributions

E. Torres: Conceptualization (equal); Data curation (lead); Formal analysis (lead); Methodology (lead); Software (lead); Validation (equal); Visualization (lead); Writing – original draft (lead); Writing – review & editing (equal). **J. Ciers:** Conceptualization (equal); Supervision (equal); Validation (equal); Writing – review & editing (equal). **S. Graupeter:** Methodology (equal); Writing – review & editing (supporting). **T. Wernicke:** Conceptualization (supporting); Funding acquisition (supporting); Project administration (supporting); Writing – review & editing (equal). **M. Kneissl:** Funding acquisition (supporting); Project administration (supporting); Writing – review & editing (supporting). Å. **Haglund:** Conceptualization (equal); Funding acquisition (equal); Project administration (equal); Resources (equal); Supervision (equal); Validation (equal); Writing – review & editing (equal).

DATA AVAILABILITY

The data that support the findings of this study are available from the corresponding author upon reasonable request.

REFERENCES

[1]M. Iwaya, S. Tanaka, T. Omori, K. Yamada, R. Hasegawa, M. Shimokawa, A. Yabutani, S. Iwayama, K. Sato, T. Takeuchi, S. Kamiyama, and H. Miyake, "Recent development of UV-B laser diodes," Jpn. J. Appl. Phys. **61**, 040501 (2022).
[2]Z. Zhang, M. Kushimoto, A. Yoshikawa, K. Aoto, L. J. Schowalter, C. Sasaoka, and H. Amano, "Continuous-wave lasing of AlGaN-based ultraviolet laser diode at 274.8 nm by current injection," Appl. Phys. Express **15**, 041007 (2022).
[3]H. Amano, R. Collazo, C. D. Santi, S. Einfeldt, M. Funato, J. Glaab, S. Hagedorn, A. Hirano, H. Hirayama, R. Ishii, Y. Kashima, Y. Kawakami, R. Kirste, M. Kneissl, R. Martin, F. Mehnke, M. Meneghini, A. Ougazzaden, P. J. Parbrook, S. Rajan, P. Reddy, F. Römer, J. Ruschel, B. Sarkar, F. Scholz, L. J. Schowalter, P. Shields, Z. Sitar, L. Sulmoni, T. Wang, T. Wernicke, M. Weyers, B. Witzigmann, Y.-R. Wu, T. Wunderer, and Y. Zhang, "The 2020 UV emitter roadmap," J. Phys. D **53**, 503001 (2020).
[4]R. Michalzik, "VCSEL fundamentals," in *VCSELs: Fundamentals, Technology and Applications of Vertical-Cavity Surface-Emitting Lasers*, edited by R. Michalzik (Springer, Berlin, Heidelberg, 2013), pp. 19–75.
[5]M. H. Memon, H. Yu, H. Jia, D. Li, R. Wang, J. Yao, Y. Kang, W. Chen, S. Li, J. Zheng, J. Zhang, C. Shen, T. Tao, B. S. Ooi, and H. Sun, "Micro-trench deep-ultraviolet LEDs with boosted efficiency for high-speed solar-blind optical communication," J. Lightwave Technol. **43**, 2248 (2025).

[6]Y. Ruan, H. Li, J. Jia, Y. Gu, Z. Zhang, D. Shen, X. Chen, Q. Li, W. Hong, X. Cui, S. Zhang, Y. Bai, and P. Tian, "High efficiency deep ultraviolet micro-LED and optical fiber coupling for low power charge management applications," Opt. Laser Technol. **181**, 111902 (2025).
[7]W. Deng, C. Jin, C. Li, S. Yao, B. Yu, and Y. Liu, "Plasma-ion-assisted deposition of HfO_2 films with low UV absorption," Surf. Coat. Technol. **395**, 125691 (2020).
[8]F. Hjort, J. Enslin, M. Cobet, M. A. Bergmann, J. Gustavsson, T. Kolbe, A. Knauer, F. Nippert, I. Häusler, M. R. Wagner, T. Wernicke, and M. Kneissl, Haglund, "A 310 nm optically pumped AlGaN vertical-cavity surface-emitting laser," ACS Photonics **8**, 135 (2021).
[9]G. Cardinali, F. Hjort, N. Prokop, J. Enslin, M. Cobet, M. A. Bergmann, J. Gustavsson, J. Ciers, I. Häusler, T. Kolbe, T. Wernicke, Å. Haglund, and M. Kneissl, "Low-threshold AlGaN-based UVB VCSELs enabled by post-growth cavity detuning," Appl. Phys. Lett. **121**, 103501 (2022).
[10]Z. Zheng, Y. Mei, H. Long, J. Hoo, S. Guo, Q. Li, L. Ying, Z. Zheng, and B. Zhang, "AlGaN-based deep ultraviolet vertical-cavity surface-emitting laser," IEEE Electron Device Lett. **42**, 375 (2021).
[11]Z. Zheng, Y. Wang, J. Hoo, S. Guo, Y. Mei, H. Long, L. Ying, Z. Zheng, and B. Zhang, "High-quality AlGaN epitaxial structures and realization of UVC vertical-cavity surface-emitting lasers," Sci. China Mater. **66**, 1978 (2023).
[12]E. Torres, J. Ciers, N. Rebelo, F. Hjort, M. A. Bergmann, S. Graupeter, J. Enslin, G. Cardinalli, T. Wernicke, M. Kneissl, and Å. Haglund, "Ultraviolet-C vertical-cavity surface-emitting lasers with precise cavity length control," Laser Photonics Rev. **19**, 2402203 (2025).
[13]J. Ciers, M. A. Bergmann, F. Hjort, J.-F. Carlin, and N. Grandjean, Haglund, "Smooth GaN membranes by polarization-assisted electrochemical etching," Appl. Phys. Lett. **118**, 062107 (2021).
[14]R. Watanabe, K. Kobayashi, M. Yanagawa, T. Takeuchi, S. Kamiyama, M. Iwaya, and T. Kamei, "Over 20% wall plug efficiency of on-wafer GaN-based vertical-cavity surface-emitting laser," Appl. Phys. Lett. **124**, 131107 (2024).
[15]T.-C. Lu, B.-S. Cheng, and M.-C. Liu, "Temperature dependent gain characteristics in GaN-based vertical-cavity surface-emitting lasers," Opt. Express **17**, 20149–20154 (2009).
[16]M. Kuramoto, S. Kobayashi, T. Akagi, K. Tazawa, K. Tanaka, T. Saito, and T. Takeuchi, "High-output-power and high-temperature operation of blue GaN-based vertical-cavity surface-emitting laser," Appl. Phys. Express **11**, 112101 (2018).
[17]L. Persson, F. Hjort, G. Cardinali, J. Enslin, T. Kolbe, T. Wernicke, M. Kneissl, J. Ciers, and Å. Haglund, "Athermalization of the lasing wavelength in vertical-cavity surface-emitting lasers," Laser Photonics Rev. **17**, 2300009 (2023).
[18]T.-C. Chang, S.-Y. Kuo, J.-T. Lian, K.-B. Hong, S.-C. Wang, and T.-C. Lu, "High-temperature operation of GaN-based vertical-cavity surface-emitting lasers," Appl. Phys. Express **10**, 112101 (2017).
[19]T. Kolbe, A. Knauer, C. Chua, Z. Yang, V. Kueller, S. Einfeldt, P. Vogt, N. M. Johnson, M. Weyers, and M. Kneissl, "Effect of temperature and strain on the optical polarization of (In)(Al)GaN ultraviolet light emitting diodes," Appl. Phys. Lett. **99**, 261105 (2011).
[20]C. Chen, P. Leisher, A. Allerman, K. Geib, and K. Choquette, "Temperature analysis of threshold current in infrared vertical-cavity surface-emitting Lasers," IEEE J. Quantum Electron. **42**, 1078 (2006).
[21]S. Kölle, F. Römer, G. Cardinali, A. Schulz, N. Susilo, D. H. Vidal, T. Wernicke, M. Kneissl, and B. Witzigmann, "Optical gain in AlGaN quantum wells: Impact of higher energy states," IEEE Photonics J. **16**, 1–5 (2024).